

BEHAVIOR AND TESTING OF SMALL SCALE COLUMNS UNDER COMBINED ACTION LOADING

NEES REU: Jennilyn M. Vallejera
Home & Host Institution: University of Nevada, Reno
REU Faculty Advisor: Dr. Sherif Elfass
REU Project Advisor: Dr. David Sanders

Abstract

The objective of this study is to verify the test setup and basic loading protocol for small scale bridge columns. Columns will be dynamically tested under combined action loading by means of a bi-axial mass rig (BMR) designed by University of Nevada, Reno (UNR) doctoral student Juan Arias. Industry design practices neglect combined action loading effects predominantly due to a lack of experimental data available. Previous studies performed bi-axially utilized quasi-static or pseudo-dynamic testing. When dynamic testing was utilized, columns were typically tested uni-axially. By performing dynamic testing on bi-axially loaded columns, it can be determined how full interactions impact the performance of bridge columns. With minimal understanding of the BMR and column interaction during testing, the significance of this study is to characterize the behavior of the testing system and column at the small scale level prior to testing at the large scale level.

Materials for the columns and BMR were selected using similitude laws given the following information: previous dynamic testing data on bridge columns and details on the proposed BMR. Construction of the small scale BMR and bridge columns are pending material testing results. Construction and testing of the system will proceed throughout the fall of 2007. At the completion of large scale testing, a comparative analysis between small scale and large scale results will be performed to verify if similitude was achieved.

TABLE OF CONTENTS

1. INTRODUCTION
 - 1.1. Project Objectives
 - 1.2. Literature Review
 - 1.3. Background of NEESR-SG Project, NSF Grant: CMS-05307337
 - 1.4. Bi-directional Mass Rig
2. SIMILITUDE LAWS
 - 2.1. Buckingham's Pi Theorem
 - 2.2. Model Selection and Column Details
3. MICROCONCRETE
 - 3.1. Concrete Mix Selection
 - 3.2. Mixing and Casting
 - 3.3. Material Testing and Results
4. BI-AXIAL MASS RIG
 - 4.1. REU BMR Details
 - 4.2. Resonance Analysis
5. ONGOING WORK: REINFORCEMENT
6. CLOSING REMARKS
7. REFERENCES
8. ACKNOWLEDGEMENTS

1. INTRODUCTION

1.1 PROJECT OBJECTIVES

The most vulnerable component of a bridge is the column. Since earthquakes inherently occur in multiple dimensions, the bridge columns too behave in a spatially complex manner in response to the earthquake (Sanders et al, 2005). This behavior is due to the physical layout of the structural system. However, industry design practice and analysis methods do not account for multi-directional behavior of the columns due to the lack of experimental data available. Of the data that is available, there exists minimal data on dynamically tested columns under combined action loading. Multi-directional studies were typically done by quasi-static or pseudo-dynamic loading; if studies were performed dynamically, they were typically done in the uni-axial direction. A bi-axial mass rig (BMR) proposed by doctoral student Juan Arias simulates torsion, bi-axial motion, and P-delta effects for the duration of dynamic testing. Because there exists no previous knowledge on how the BMR and column will behave when tested at the large scale, this project aims to create a small scale BMR and columns to test prior to testing at the large scale.

1.2 LITERATURE REVIEW

Vertical Motion Effects

A study by Papazoglou and Elnashai (1996) states that some structural failures can be primarily attributed to the vertical component of ground motion, although most are attributed to flexural failure modes. Overlooking vertical motions eradicates the possibility of failure caused by the variation in axial loading on the structure. Columns in mild tension or reduced compression have the tendency to erode shear strength of the column (Papazoglou and Elnashai, 1996). Data recorded at Castaic Old Ridge during the 1971 San Fernando earthquake shows that shear failure is likely when accounting for vertical ground motion; it also verifies higher variation in axial loads in upper stories of a structure. Figure 1 demonstrates that demand exceeds capacity repetitively throughout the analysis, and since the frequency of the demand is not very high, it cannot be over looked, according to a study by Papazoglou and Elnashai (1996).

Additionally, a study at Imperial College was completed on vertical motion effects on a hypothetical asymmetrical RC bridge designed to withstand a 0.5g event. Figure 2 displays the need for refinement in the commonly used ratio (a_v / a_h) of vertical to horizontal peak ground acceleration of $2/3$ at varying points where demand exceeds shear capacity (Sanders *et al*, 2005). Shear failure of the squat column within the RC bridge was only encountered when vertical motion was combined with horizontal excitation.

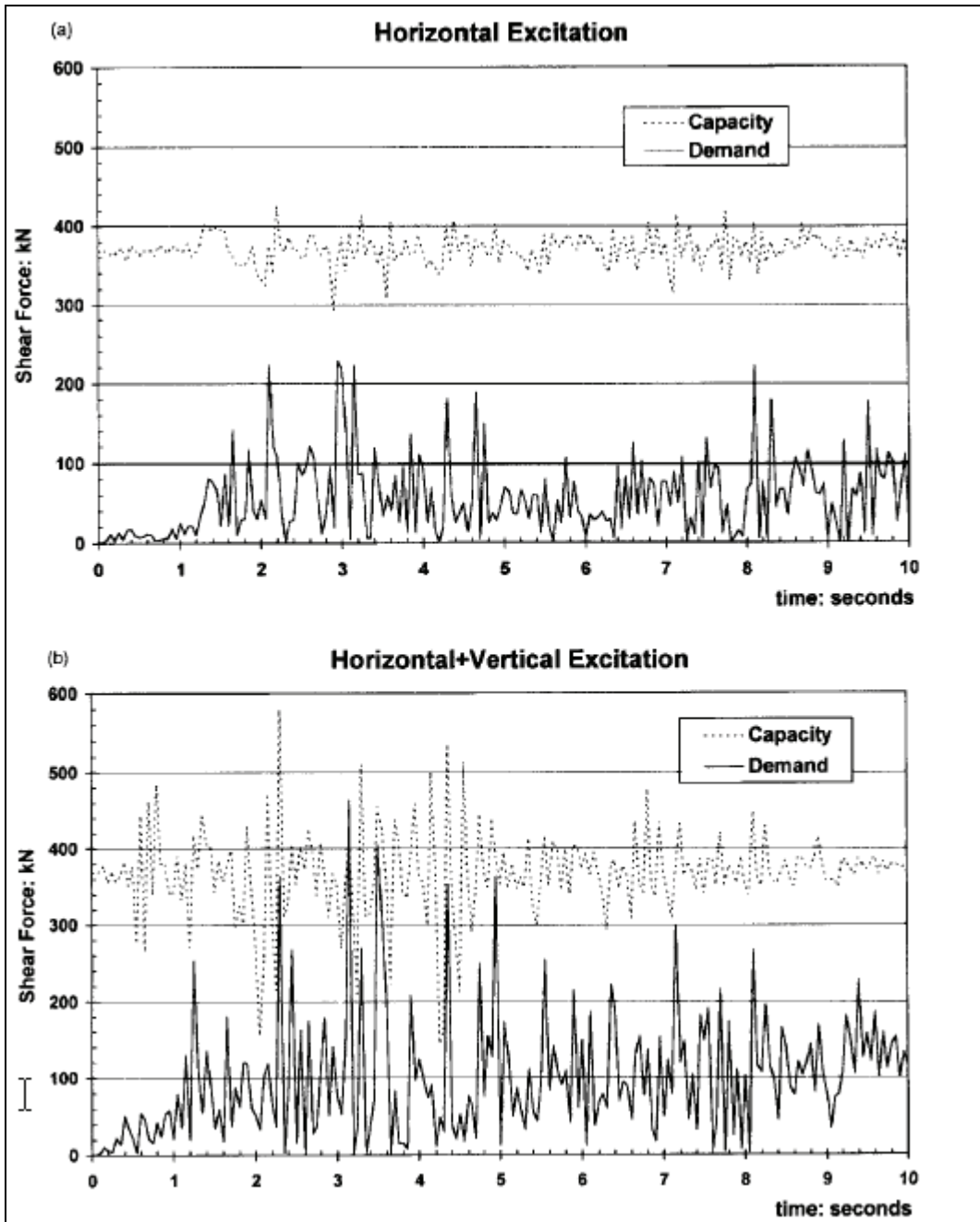


Fig. 1. Effect of varying components of motion on axial force response reproduced from Broderick et al, 1995

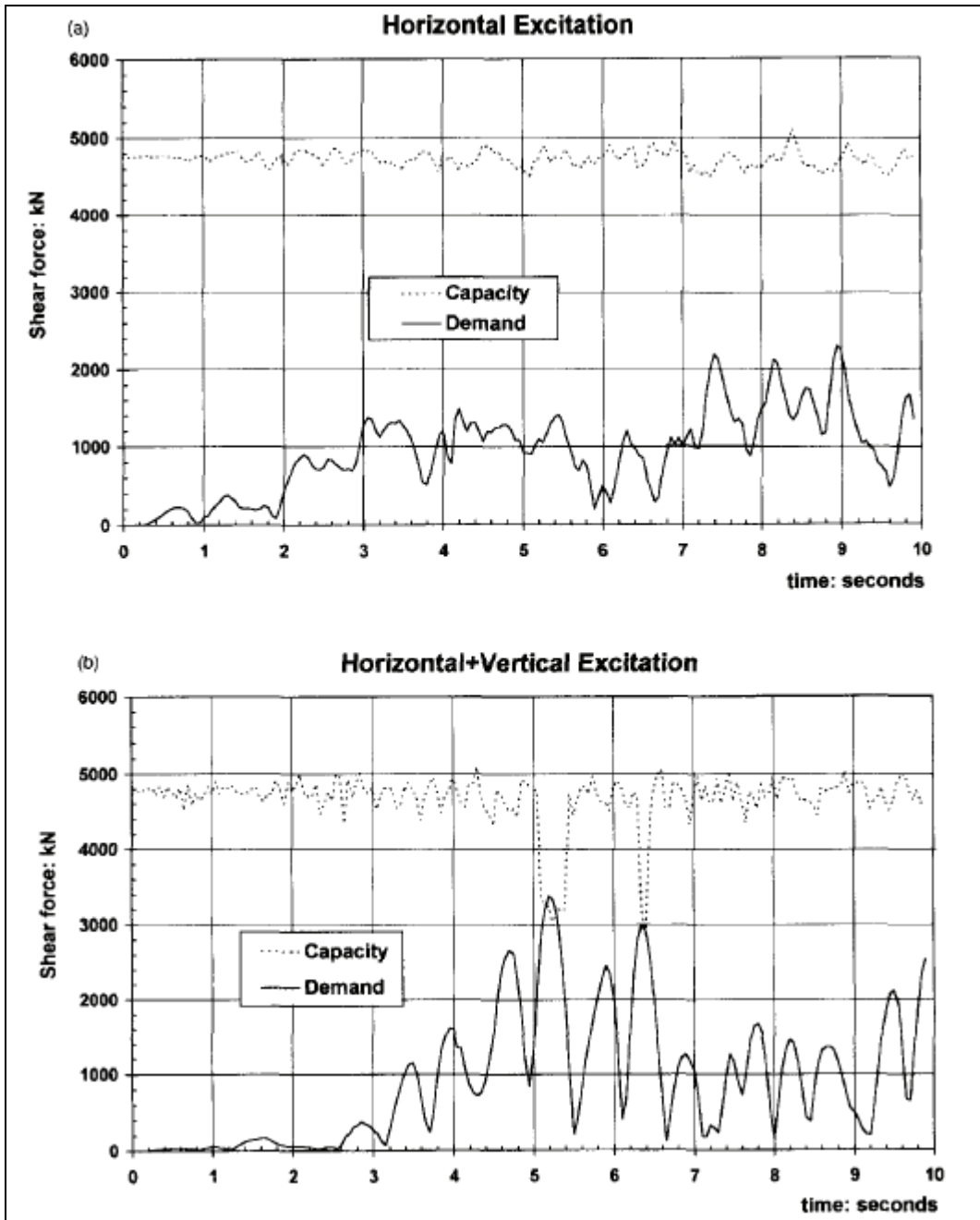


Fig. 2. Shear capacity and demand time-histories for an asymmetric curved RC bridge under horizontal and horizontal-vertical excitation produced using data from Dodd et al, 1994

Torsional Effects

Torsion occurs due to the spatial layout of the structure including the eccentricity of inertia causing torsion transference from superstructure to substructure and abutment and deck pounding of skewed bridges (Sanders et al, 2005). Because of the irregular shape of the structure, complex flexure and shear failures occur. Using a dynamic testing facility at the Tokyo Institute of Technology, tests were performed simulating cyclic bending, torsion, and a combination between the two. A rotational-drift ratio was utilized to control the level of bending and torsion applied, where θ is the rotation of the column in radians and Δ is the lateral drift at the effective height of the column (Tirasit and Kawashima, 2006):

$$r = \theta / \Delta \tag{1.1}$$

Columns tested individually with cyclic bending or cyclic torsion had different hysteresis curves in comparison to combined cyclic bending and torsion in spite of varying rotational-drift ratios. In Fig. 3, as r increases, the flexural strength, stiffness, and lateral restoring force deteriorate. Additionally, as r approaches 1, torsion capacity of the column deteriorates; this indicates brittle failure of torsion when the column is under cyclic bending and torsion when $r \geq 1$.

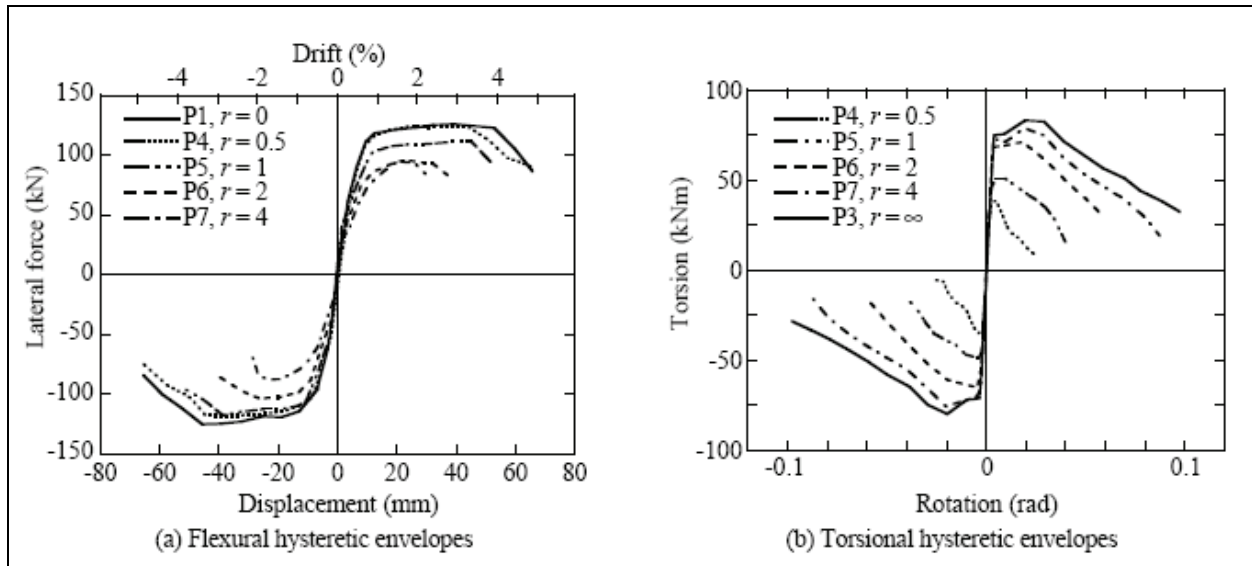


Fig. 3. Summary comparison of hysteretic envelopes provided by Tirasit and Kawashima, 2006.

1.3 NEESR-SG PROJECT, NSF GRANT#: CMS-05307337

The objective of NEESR-SG project is to determine the impact of performance and system response on bridge columns under combined actions, and in addition, to determine analysis and design procedures that account for the impact. In collaboration with six other institutions, real-time dynamic testing of 12 large scale columns with bidirectional, torsional, and variable axial load inputs will be completed at UNR.

In 1999, real-time dynamic testing in the uni-axial direction was performed utilizing a SDOF mass rig proposed by Patrick Laplace. The BMR proposed was based conceptually on the SDOF mass rig. The columns designed were 1/3 scale in relation to the prototype and will be replicated for the 12 large scale columns; the axial load and steel ratios used for the columns are typical of CALTRANS design.

1.4 BI-DIRECTIONAL MASS RIG

Through the BMR, the inertial mass will be simulated and supported by the deck of the structure rather than placed directly on top of the column. Unlike the SDOF mass rig, the BMR will act directly on the shake table to simulate torsion and bidirectional motion through eight pins. At the interface between the shake table and supporting columns of the BMR, ball joint rod ends will allow for bidirectional and torsional capability, where rotation limitations in one direction will be approximately 10 degrees. Limitations on translation of the BMR will be pre-set to chosen displacement values by restraining cables in both directions. The inertial mass on the deck of the BMR can be logistically placed as needed to simulate desired effect. The attachment of BMR to column is created by links pin connected at either end to simulate shear. Figure 4 displays the BMR.

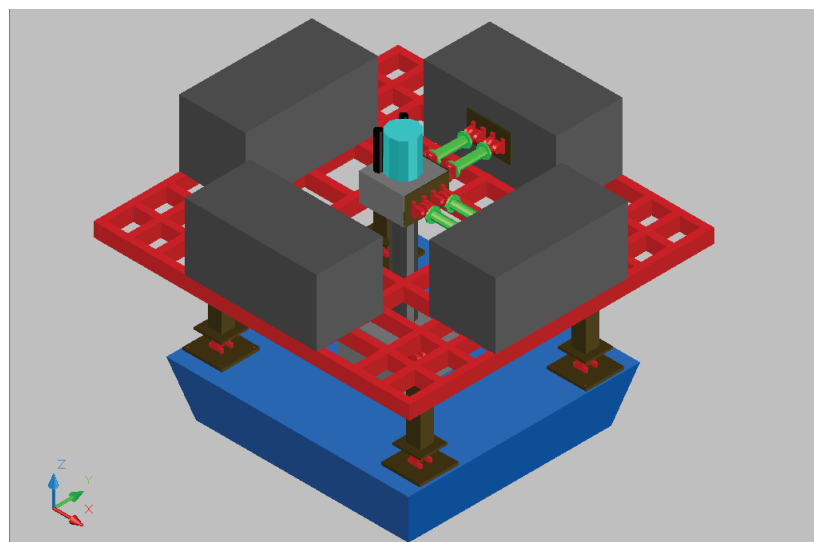


Fig. 4. Bi-directional mass rig proposed by Juan Arias

2. SIMILITUDE LAWS

2.1 BUCKINGHAM'S PI THEOREM

Scaled modeling is not uncommon in engineering experiments. Using scaled modeling in experiments typically arises from economic feasibility and/or limited laboratory capabilities (Holub, 2005). However, small scale modeling is often matched with unwarranted skepticism concerning accuracy; when materials, loading protocol, and instrumentation is adequately accounted for, testing at the small scale can provide accurate results (Moncarz and Krawinkler, 1981). For scaled modeling, the basic concepts of scaling derive from Buckingham's Pi Theorem of 1914, which states the following (Holub, 2005):

If an equation involving n variables is dimensionally homogeneous, it can be reduced to a relationship among $n-k$ independent dimensionless products, where k is the minimum number of reference dimensions required to describe the variables involved.

Essentially, the n number variables of the prototype problem are expressed in terms of x and can be transformed into dimensionless products expressed in terms of π . This can also be applied to the model to be tested. Should the resulting π products of the prototype be set equal to the model such that:

$$\pi_{2p} = \pi_{2m}, \pi_{3p} = \pi_{3m}, \dots, \pi_{(n-k)p} = \pi_{(n-k)m} \quad (2.1)$$

Then it follows that the two structures are thus similar, resulting in the following (Holub, 10):

$$\pi_{1p} = \pi_{1m} \quad (2.2)$$

It must be stated that caution should be taken into the selection of variables accounted for in the problem. Not accounting for enough variables to the problem will lead to incorrect results, but accounting for too many variables will apply unnecessary restraints to the problem (Moncarz and Krawinkler, 1981). For the REU project, scale factors were determined using Buckingham's Pi Theorem, and Table 1 summarizes the various relationships between the model scale chosen and the different variables accounted for (Laplace, 1999).

Table 1. Model scale factors.

Length	l_r
Area	l_r^2
Stress	1.0
Mass	l_r^2
Force	l_r^2
Strain	1.0
Displacement	l_r
Acceleration	1.0
Time	$l_r^{1/2}$
Period	$l_r^{1/2}$
Moment	l_r^3

2.2 MODEL SELECTION AND COLUMN DETAILS

The REU model scale was selected based on the decision to utilize a 3-inch diameter column for testing, whereas the UNR model utilized a 16-inch diameter column. Thus, a 3/16 scale was selected for the REU research project through the model scale factors of Table 1. To ensure a flexural response, an aspect ratio of 4.5 was maintained from the UNR model. In addition, the axial load ratio, longitudinal steel ratio, and spiral ratio maintained from the UNR model requirements were 0.10, 0.02, and 0.01, respectively. Table 2 summarizes the dimensional characteristics of both columns including the chosen reinforcement bars and spacing for the longitudinal direction and for confinement as well.

Table 2. Column details.

	UNR MODEL	REU MODEL
Scale	1	3/16
Column Height	72. in	13.5 in
Column Diameter	16.0. in	3.0. in
Axial Load	80.4 kips	2.8 kips
Long. Bars	#4 - 20 bars	W2 - 8 bars
Confinement	0.25 in Ø wire	0.039 in Ø wire
Spiral Pitch	1.5 in	0.19 in
Concrete Cover	0.67 in	0.13 in

To ensure that the REU model was scaled accurately, a moment-curvature analysis was performed utilizing XTRACT, a cross-sectional analysis program. The UNR and REU models were compared by failure and ultimate moment values to verify if the column details of the REU model were similar to that of the UNR model. As shown in Figs. 5 and 6, the materials for both columns fail similarly.

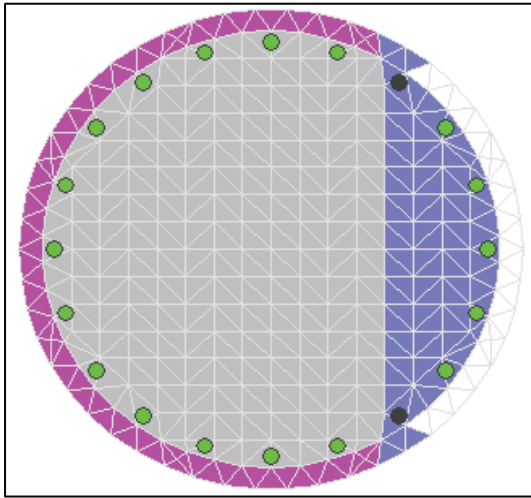


Fig. 5. UNR 16-in diameter model

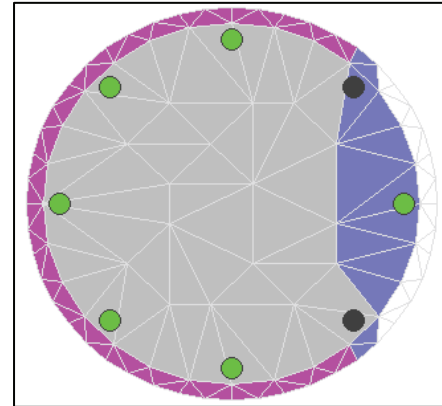


Fig. 6. REU 3-in diameter model

During the uni-axially testing of the UNR columns, peak lateral forces of 32.3 kips and 35 kips were attained; the columns were subjected to incrementally increasing ground accelerations and initial large motion followed by two aftershocks, respectively. Based on the peak lateral force values, the ultimate moment capacity ranged within 2,320 in-kips – 2,520 in-kips. In Fig. 7, the UNR model in XTRACT performed as tested. From Fig. 8, the REU model performed as expected using the moment scale factor calculation. The discrepancy in the moment-curvature plot past the yield point for the REU model can be attributed to the limitation in mesh size within the program. XTRACT discretizes the cross-section into triangular meshes to analyze, and the mesh size specified is the average length of the side or fiber of each triangle, typically 1/16 of the smallest dimension of the specimen. An error is generated when the number of fibers exceeds the maximum value provided; however, the more triangular meshes created, the more accurate the analysis results provided. Figure 8 displays the smallest allowable mesh size used for moment-curvature analysis.

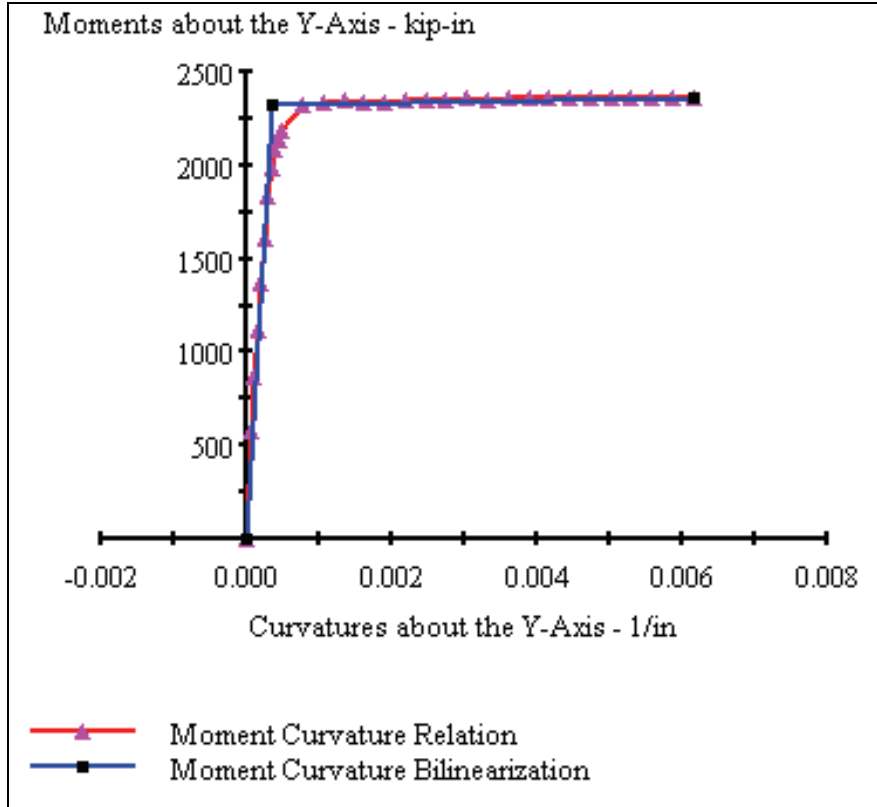


Fig. 7. Moment-curvature curve for UNR model.

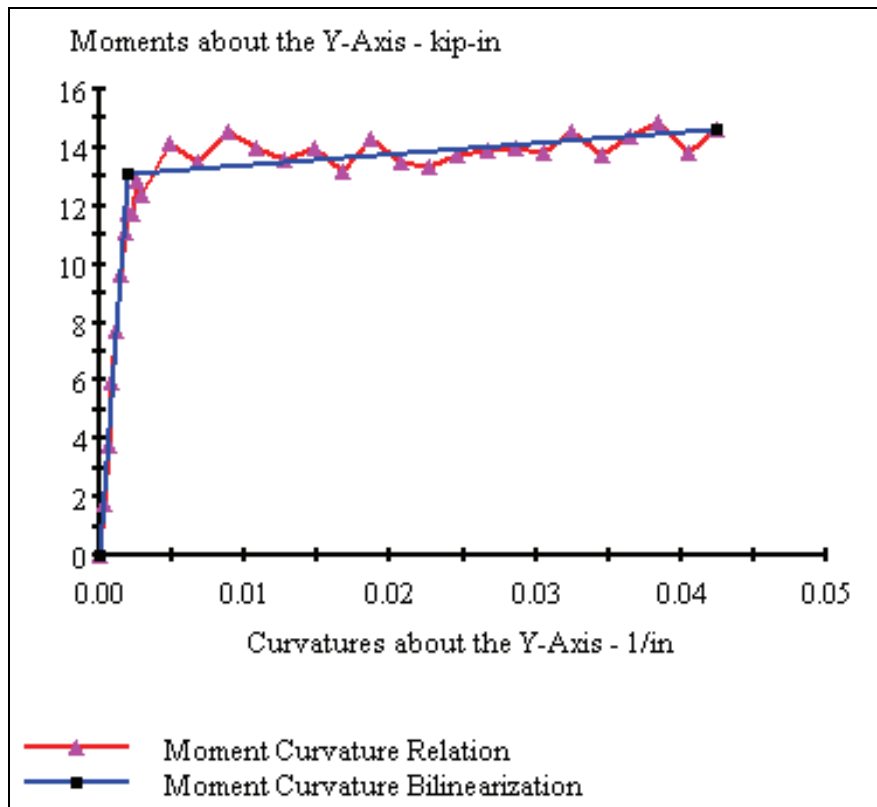


Fig. 8. Moment-curvature curve for REU model.

3. MICROCONCRETE

3.1 CONCRETE MIX SELECTION

Microconcrete is a concrete mix using a scaled aggregate gradation to partially fulfill similitude criteria. In terms of similitude, the expectation is to have the scaled concrete mix duplicate the stress-strain response of the model under any given stress state imposed (Holub, 2005). However, meeting that criterion would be difficult if not impossible. Instead, because compressive strength is of utmost importance for concrete, compressive strength and stress-strain response in compression are the basic criteria in which the model must match the prototype, followed by tensile strength and time-dependent behavior (Harris and Sabnis, 1999).

Holub tested eight different mix designs of microconcrete, varying the water-cement and aggregate-cement ratios for each mix, with no addition of admixtures. Since the target compressive strength was the same for this project, three mixes were selected for replication based on results of workability. Based on the given ratios, components in terms of weight of the microconcrete mix – water, aggregate, and cement – were determined (Table 2).

Table 2. Summary of microconcrete mixes

A/C Ratio:	2.5	3.25	2.25
W/C Ratio:	0.5	0.5	0.55
Coarse Aggregate (>6.3mm):	0	0	0
Fine Aggregate (<6.3mm):	9.375 #	10.26 #	8.88 #
Water:	1.875 #	1.58 #	2.17 #
Cement:	3.75 #	3.16 #	3.95 #
Air:	0	0	0

Holub utilized a local source of crushed limestone and did not specify material properties required for the microconcrete mixes trialed. Thus, the aggregate utilized for the REU project was Lockwood Wade Sand (LW-WS), a local source in Reno provided by the UNR pavements laboratory. LW-WS was tested for moisture content and absorption through AASHTO T-84 and yielded 0.74% and 1.3%, respectively. To ensure replication of the mix, the same gradation utilized by Holub was utilized for the three chosen mixes. Figure 9 displays the gradation utilized for both studies. In addition, although Holub used Type III cement, Type I was applied to the microconcrete mixes since it was readily available and provided by the UNR materials lab. Type III cement is typically employed only to expedite the compressive strength of concrete for studies and creates no distortion in comparison to Type I cement in the final concrete product (Holub, 2005).

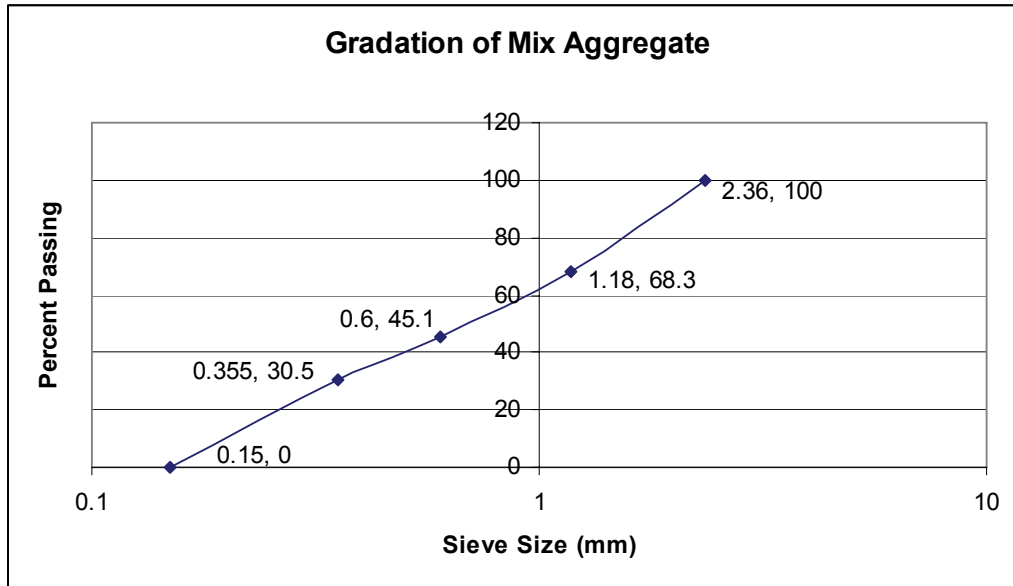


Fig. 9. Aggregate gradation for microconcrete mix.

3.2 MIXING AND CASTING

Mixing

The volume of the mixes was scaled up approximately 20% to ensure an adequate amount would be available. Scaling up the amount of needed mix aided in homogenous mixing of the individual components in a standard table mixer. Caution was taken to ensure the volume of material required for the mix would be less than 75% the capacity of the table mixing bowl enabling full incorporation of materials within the mix. The following was employed for mixing the microconcrete:

- 1) 10% of each individual component – water, aggregate, cement – is mixed for 1 minute to promote uniform mixing for the ingredients.
- 2) Liner mix is discarded; mix remaining 90% of materials for 2 minutes. Figure 10.
- 3) The table mixer is stopped for 1 minute.
- 4) The mixing is repeated for another 2 minutes.



Fig. 10. Standard table mixer and microconcrete mix.

There exists no code or specification to determine the workability of microconcrete. To have a standard testing means to determine the workability of the various mixes, Holub utilized the ASTM test which characterizes fine aggregate absorption. This method was adopted for this study in order to compare workability values. The cone and rod utilized for the test were designated in ASTM C70 and ASTM C143, respectively. The following procedure was utilized to determine workability (Holub, 2005):

- 1) The cone is placed with the largest diameter end resting on a smooth surface.
- 2) The cone is filled in two lifts of microconcrete, rodded 5-10 times per lift.
- 3) The cone is struck off and excess microconcrete surrounding the cone is disposed.
- 4) The cone is slowly lifted, inverted, and placed adjacent to the microconcrete.
- 5) The slump is measured with respect to the adjacently placed cone. (Figure 11.)



Fig. 11. Workability test.

ASTM provides testing procedures to determine the compressive and tensile properties of concrete, but there exists no such procedure for microconcrete. Because the aggregate was scaled to create the microconcrete, utilizing a standard 6-in x 12-in cylinder as a test specimen for determining the strength properties of the mix would be highly inaccurate. Size effects can be thought of as a change in indicated strength due to a change in specimen size (Holub, 2005). ACI attempted to alleviate this issue in a report by recommending the usage of 2-in. x 4-in. cylinders as the standard testing specimen for model studies (ACI, 1979). In addition, the ACI noted that additional cylinders may be required for testing very small concrete mixes, but this does not affect the project at hand since the smallest characteristic dimension of the columns of concern is 3-inches, exceeding the 2-in diameter of the ACI specified specimen.

After mixing, the microconcrete was placed in 2-in x 4-in disposable cylinders. Again, no standard procedure exists for air removal from microconcrete cylinders; thus, the following procedure was employed:

- 1) Pour 2-in of microconcrete in cylinder.
- 2) Rod 10-15 times with the end of a pencil eraser.
- 3) Pour the remaining 2-in of microconcrete in cylinder.
- 4) Rod 10-15 times with the end of a pencil eraser.

- 5) Tap edge of the cylinder with a tamping rod 15 times with cylinder placed on a flat surface.
- 6) Strike off excess on top of cylinders and cap.

3.3 MATERIAL TESTING AND RESULTS

Twenty-seven cylinders were created, nine per each mix. The cylinders were immediately placed in the UNR moisture room and removed after four days; specimens were removed from the disposable cylinder encasements on day thirteen. Three cylinders per mix were tested for f'_c to determine 14-day compressive strength, and the results are listed in Table 3. Three cylinders per mix will be tested for f'_c to determine 28-day compressive strength, and the remaining cylinders will be tested for tensile strength (f'_t) on the same day. The mix selected for testing will be determined on the basis of f'_c and f'_t values that approximate the strength properties of the UNR columns, 5,000 psi and 510 psi, respectively.

Table 3. 14-day compressive strength of microconcrete mixes.

	Compressive Stress (psi)	f'_c (psi)
Mix 1		5172
1A	5250	
2A	5110	
3A	5155	
Mix 2		4260
1B	4060	
2B	4135	
3B	4585	
Mix 3		4552
1C	4070	
2C	4835	
3C	4750	

4. BI-AXIAL MASS RIG

4.1 REU BMR DETAILS

Utilizing the information provided by Juan Arias, the materials for the REU BMR were scaled using the model scale factor table in Table 1. The materials to comprise the REU BMR are compared to the proposed BMR and summarized in Table 4.

Table 4. REU BMR materials list.

Quantity	Materials for Mass Rig	Size for UNR BMR	Size for REU BMR
10	Deck Beams	HSS 10x5x1/4	2x1x1/16
4	Column Supports	HSS 8X8X1/2	1.5sqx1/10
16	Swivel	50-kip dynamic rod end	5-kip ball joint rod end
4	Link Beams	HSS 6x6x1/2	1.25sqx1/10

4.2 RESONANCE ANALYSIS

Testing on the shake table requires resonance analysis to ensure that the REU BMR will behave as anticipated and can be controlled. The UNR shake table has a resonant frequency of 13 Hz. If the modal frequencies of the BMR and column far exceed 20 Hz, control of REU BMR will be impossible and the REU BMR will not move. If the modal frequencies range within the target resonant frequency of the shake table, the system is expected to have an exaggerated behavior, but experience working with the shake table has enabled the structures laboratory manager to use parameters to avoid such effects. Values considerably below the resonant frequency of the table are not of concern. Thus, a modal analysis was performed on the REU BMR and column in SAP2000 to determine the modes of the system and to verify that unforeseen resonance difficulties will not be encountered on the shake table.

Additionally, various mode shapes were taken into consideration when looking at the frequencies of the 12 modes identified. The majority of modes were considered warped modes where warping would occur at the deck of the REU BMR. Also, some mode shapes only affected the deck by the mass loads applied for inertial mass simulation. Both types of mode shapes were neglected in this analysis. Mode shapes of concern were those acting uni-axially in the direction of the actuators or mode shapes simulating torsion or bi-axial movement.

Information required for modeling included the following: dimensional and material properties of both the column and REU BMR, joint details to interface the column to the REU BMR, and joint constraints applied to the masses on the deck of the REU BMR. Table 5 summarizes the modal analysis results; based on frequency and mode shape combined, the table shows that resonance will not be an issue during testing.

Table 5. Modal periods and frequencies from SAP analysis.

TABLE: Modal Periods And Frequencies		
StepNum	Period	Frequency
Unitless	Sec	Cyc/sec
1	0.391065273	2.56
2	0.218278514	4.58
3	0.218217229	4.58
4	4.81E-02	20.81
5	2.97E-02	33.69
6	2.82E-02	35.41
7	2.49E-03	401.72
8	2.17E-03	459.93
9	1.43E-03	698.71
10	1.33E-03	750.30
11	1.27E-03	787.37
12	1.23E-03	811.41

5. ONGOING WORK: REINFORCEMENT

Grade 60 steel is standard for rebar. However, the reinforcement required for the REU columns are considerably smaller than #3 bar – the smallest standard rebar size – and therefore alternative materials for reinforcement must be used. Typically, various types of wire have been utilized in model testing. Common sizes of wire were specified by Appendix E in the ACI Building Code and Table 1 was used to calculate the required diameter for reinforcement (2005). Comparing calculated results to wire size specified in the ACI, the longitudinal reinforcement required W2 wire and the transverse spiral hoop used for concrete confinement required a wire diameter of 0.039-inches (1-mm).

To partially fulfill similitude laws, the modulus of elasticity, yield point, and yield plateau are typically modeled (Holub, 2005). Two primary types of wire tested by Holub were smooth wire and commercially available deformed wire. Smooth wire is typically used where bond development is not an issue, particularly in areas of shear. Consequently, smooth wire has been selected as the material for transverse reinforcement. Threaded rod, a commercially available material, has been selected for longitudinal reinforcement.

The stress-strain response of wires is typically ill-defined. However, various heat treatment processes are widely available to normalize or to lower and re-establish a well-defined yield point (Holub, 2005). The material tests will determine the tensile strength of each type of wire before and after heat treatment using an Instron extensometer following the procedures of testing used by Holub. Another issue of concern is bond development between longitudinal reinforcement and microconcrete. Threaded rod is hypothesized to exhibit high bond strength, but there is not data available quantifying the difference between prototype and model. This problem requires further research to determine how to achieve similitude in longitudinal reinforcement.

6. CLOSING REMARKS

Similitude laws have been utilized throughout this project to acquire the materials needed to create a small scale BMR and columns with respect to the prototype, the UNR BMR, and columns. Testing of the three microconcrete mixes is still in progress; a mix will be selected after the average compressive and tensile strengths at 28-days have been determined. When the materials for the REU columns have been selected and construction of the REU BMR is completed, testing of the REU columns will follow. A comparative analysis will be done between the REU BMR test and the large scale BMR test at the finish of large scale testing. It is anticipated that work on this project will continue on throughout the fall of 2007.

7. REFERENCES

1. ACI Committee 444: Models of Concrete Structures, (1979), "Models of Concrete Structures – State-of-the-Art," *Concrete International*. Jan. 1979.
2. ACI, 2005. *Building Code Requirements for Structural Concrete (ACI-318-05) and Commentary (ACI 318R-05)*, American Concrete Institute, Farmington Hills, MI.
3. ASTM, 2005. *Manual of Aggregate and Concrete Testing*. American Society for Testing and Materials, West Conshohocken, PA.
4. Broderick, B. M. and Elnashai, A. S. (1995), "Analysis of the failure of the Interstate 10 freeway ramp during the Northridge earthquake of 17 January 1994," *Earthquake eng. struct. dyn.* 24, pp. 189-208.
5. Dodd, S. G., Elnashai, A. S., Izzuddin, B. A. and Calvi, G. M., "A 3-D nonlinear time-history analysis of a curved bridge," in R. Park (ed), *Seismic design and retrofitting of reinforced concrete bridges*, Proc. Second Int. Workshop, Queenstown, New Zealand, 1994, pp. 61 7-639.
6. Elnashai, A.S. and Papazoglou, A.J. (1997), "Procedure and spectra for analysis of RC structures subjected to strong vertical earthquake loads," *Journal of Earthquake Engineering* 1997, vol.1, pp. 121-155.
7. Harris, H.G., Sabnis, G.M., (1999), *Structural Modeling and Experimental Techniques*, CRC Press, Boca Raton.
8. Holub, C.J., "Similitude considerations for small scale distributed hybrid testing of reinforced concrete bridges," Master of Science Thesis, University of Illinois at Urbana-Champaign, 2005.
9. Laplace, P., D. H. Sanders, M. Saiidi, and B. Douglas, "Shake Table Testing of Flexure Dominated Reinforced Concrete Bridge Columns", Civil Engineering Department, University of Nevada, Reno, Report No. CCEER-99-13, December 1999.
10. Moncarz, P.D. and Krawinkler, H. (1981), "Theory and Application of Experimental Model Analysis in Earthquake Engineering." John A. Blume Earthquake Engineering Center technical report. No. 50. Stanford University.
11. Sanders, D.H., Belarbi, A., Zhang, J., Dyke, (2005), "Seismic Simulation and Design of Bridge columns under combined Actions and Implications on System Response," National Science Foundation Research Grant CMS-05307337.
12. Tirasit, P. and Kawashima, K.(2006), "Combined Cyclic Flexural-Torsional Loading Test of RC Columns," *Journal of Structural Engineering*, 52A, pp.437-443.

8. ACKNOWLEDGEMENTS

As part of the 2007 Network for Earthquake Engineering Simulation (NEES) Research Experience for Undergraduates (REU), research was conducted. Funding was provided by the National Science Foundation. Special thanks to my REU advisor Dr. David Sanders for his guidance throughout every step of my project and for giving me the opportunity to partake in the program. Thanks to Dr. Sherif Elfass, Dr. Gokan Peckan, Dr. Patrick Laplace, Dr. Candice Bauer, Rita Johnson, Curtis Holub, Paul Lucas, and Juan Arias for their assistance. Finally, thank you to REU's Austin Brown and Alex Piolatto for aiding me in my project endeavors.